Non-Hermitian Engineering of Synthetic Saturable Absorbers for Applications in Photonics

M. H. Teimourpour,[1,2] A. Rahman,[1,2] K. Srinivasan,[3] and R. El-Ganainy[1,2,*]

[1]*Department of Physics, Michigan Technological University, Houghton, Michigan 49931, USA*
[2]*Henes Center for Quantum Phenomena, Michigan Technological University,*
Houghton, Michigan 49931, USA
[3]*Center for Nanoscale Science and Technology, National Institute of Standards and Technology,*
Gaithersburg, Maryland 20899, USA

We explore a type of synthetic saturable absorber based on quantum-inspired photonic arrays. We demonstrate that the interplay between optical Kerr nonlinearity, interference effects, and non-Hermiticity through radiation loss leads to a nonlinear optical filtering response with two distinct regimes of small and large optical transmissions. More interestingly, we show that the boundary between these two regimes can be very sharp. The threshold optical intensity that marks this abrupt "phase transition" and its steepness can be engineered by varying the number of the guiding elements. The practical feasibility of these structures as well as their potential applications in laser systems and optical signal processing are also discussed.

I. INTRODUCTION

The emerging field of non-Hermitian photonics [1–7] offers many new opportunities for building photonics devices with novel functionalities such as single-mode lasers [8–12], exceptional point-based sensors [13], as well as light sources based on non-Hermitian phase matching [14]. An area that still remains largely unexplored (apart from the work in Ref. [6] and the recent results in Refs. [10–12,14]) is the engineering of the nonlinear non-Hermitian response function of photonic structures to achieve useful functionalities. In this work, we explore one such possibility and we provide a photonic geometry that exhibits a saturable absorber response with superior performance. As we will explain in detail shortly, in our system the non-Hermiticity arises from the interplay between discrete diffraction, Kerr nonlinearity, and optical loss due to the coupling of light to the electromagnetic continuum.

Saturable absorbers (SA) are optical components that exhibit large or small optical-absorption coefficients at low or high light intensity, respectively [15]. They are indispensable tools for a wide range of applications from mode locking [16,17] and Q switching [16,17] to pulse shaping and stabilization [18,19] and noise suppression [20]. In general, saturable absorbers can be classified into two main categories based on their operation principle: (1) devices that rely on engineered electronic band structures to achieve proper functionality and (2) artificial saturable absorbers that exhibit a decrease in optical absorption at high intensities without having physical absorption saturation. Semiconductor SA mirrors [21], quantum-dot-based SA [22], and SA that utilize

the optical and electronic properties of carbon nanotube [23] and graphene [24] are examples of the former. The latter includes Kerr lensing [25], fiber loops [26], and nonlinear waveguide arrays [27].

In particular, using uniform waveguide arrays as artificial saturable absorbers utilizes the interplay between Kerr nonlinearity, which is an intrinsic property of the material, and discrete diffraction which can be engineered by scaling the uniform coupling coefficients between the guiding channels [28]. This strategy has been used to investigate mode locking using waveguide arrays [29–31]. In the past few years, different types of nonuniform waveguide arrays have been proposed and shown to exhibit interesting features. A particular structure that received considerable attention recently is the so-called J_x array [32–36]. Among the intriguing characteristics of J_x photonic arrays is coherent transport between ports that are related through mirror reflection around the array's axis of symmetry [32]. This feature was recently utilized in a theoretical proposal to build on-chip optical isolators and polarization beam splitters [37,38]. In addition, due to their ladder eigenvalue spectrum, revival effects have been also recently predicted in supersymmetric partners of J_x arrays [39], despite the fact they do not possess any spatial symmetry.

II. SYNTHETICS SATURABLE ABSORBERS IN J_x ARRAYS

To date, nonlinear light interactions inside J_x arrays have not been investigated. In this paper, we consider the effect of Kerr nonlinearity on light propagation in J_x arrays and we show that under the appropriate conditions, these structures can function as a synthetic digital saturable absorber, i.e., as a SA with an extremely sharp transition
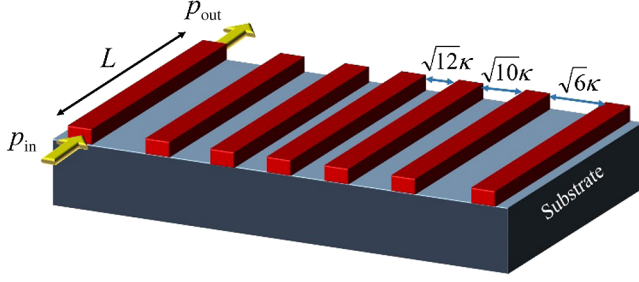
*ganainy@mtu.edu

FIG. 1. Schematic of a nonlinear J_x array made of seven waveguide elements. The coupling profile is symmetric around the central channel and values of the coupling coefficients are indicated. The array length $\xi = L \equiv \pi/2$ is chosen to provide coherent perfect transfer under linear conditions. The Kerr nonlinear coefficient in these arrangements is a function of the material properties and the mode confinement inside the waveguide. In our proposed saturable absorber scheme, light is launched in and collected from in the leftmost port. The other additional ports serve as a mean to introduce optical loss either by direct radiation into free space or by introducing physical loss as explained in the text.

between the low- and high-transmission regimes as a function of the input optical intensity.

Figure 1 depicts a schematic illustration of a photonic J_x waveguide array. Within the coupled mode formalism, continuous-wave light propagation inside a J_x array having a total number of guiding elements equal to $2N + 1$ (with N being integer or half-integer number) is given by

$$i\frac{dE_n}{dz} + \kappa(g_{n-1}E_{n-1} + g_n E_{n+1}) + \chi|E_n|^2 E_n = 0. \quad (1)$$

In Eq. (1), E_n is the electric-field-envelope amplitude in waveguide $n \in [-N, N]$, z is the propagation distance, while κ is a scaling constant that characterizes the coupling between the different elements, and the coupling profile is given by $g_n = \sqrt{(N+n)(N-n+1)}$, $g_{-N} = 0$, and $g_{N+1} = 0$ (see Refs. [32–38,40] for a detailed derivation of the coupling profile g_n). Furthermore, χ is the effective nonlinear Kerr coefficient and it is proportional to the material nonlinearity and the optical-mode confinement factor [41]. Figure 1 depicts a schematic of a J_x array made of seven waveguides ($N = 3$). The input and output ports of the device are also indicated on the figure. The additional output ports serve as a means for introducing optical losses to the system by coupling the undesired light components in these channels to the radiation continuum. In practice, depending on the modal profile and phase mismatch between the waveguide modes and free-space propagation, a small fraction of this light will be reflected and transmitted back to the input channel. This feedback process might hamper the operation of the device. This can be overcome by extending the auxiliary ports beyond the device length, bending them away from the main port, and

introducing physical optical absorption on each channel through metal deposition. These design details will be explored in future studies.

We proceed by using the scaling $\xi = \kappa z$ and $E_n = \sqrt{P_o} a_n$, where ξ and a_n are the normalized distance and field amplitude, respectively, while P_o represents the input optical power. We finally obtain $i[(da_n)/d\xi] + (g_{n-1}a_{n-1} + g_n a_{n+1}) + \alpha|a_n|^2 a_n = 0$, where the nonlinear parameter is given by $\alpha = \chi P_o/\kappa$. Under linear conditions, when $\alpha = 0$, light propagation in these arrays undergoes coherent transport where an optical beam launched in one port will exit from the mirror symmetric port with a unit power transmission [32] after a certain propagation distance. As a result, in this case, the transmission coefficient between input and output ports T belonging to the same channel (leftmost waveguide in Fig. 1) will be zero. When the input light intensity is increased, or equivalently by increasing α, the transmission coefficient T is expected to grow as the nonlinear self-trapping effects start to overcome discrete diffraction [28]. These intuitive predictions are confirmed in Fig. 2(a), where we plot the values of T as a function of the nonlinear coefficient α or, equivalently, the input light intensity for three different J_x arrays made of three, seven, and eleven guiding elements, respectively. In all arrangements, the input light is launched in the leftmost waveguide. The normalized length of each J_x array is chosen to be $\xi = L \equiv \pi/2$ in order to produce exactly zero transmission when $\alpha = 0$ (see Ref. [28], and references therein). Interestingly, we observe a very sharp transition between the low- and high-transmission states (off and on states) as a function of the nonlinear parameter α. In addition, the location at which this transition takes place, α_{TH} defined as the threshold value of α at which the transmission starts to rise above, say, 5×10^{-3} monotonically (alternatively one might chose other criteria for α_{TH} such as the point where the slope of the curve changes to a certain value), is a function of the waveguide number. For comparison, we also study the dynamics in uniform waveguide arrays. If the array is infinite, the uniform coupling κ_u can be chosen to produce exact zero transmission under single excitation conditions after a propagation distance of L, i.e., it satisfies the relation $J_o(2\kappa_u L) = 0$, where $J_0(x)$ is the Bessel function of order zero and argument x (see Ref. [28] for discussion, and references therein for a detailed derivation). A large but finite array can still exhibit near-zero linear transmission similar to an infinite array if we maintain the above condition and launch light only in the central channel. Figure 2(b) shows the transmission curves for uniform arrays made of three, seven, and eleven waveguides when light is launched in the central element of the array. Clearly, the transition between the two regimes in this latter case is less abrupt than in the case of the J_x array (the slope of the curve for a uniform array with eleven waveguides is ∼10% of that of the case of a J_x array having the same number of channels). Finally, for completeness,
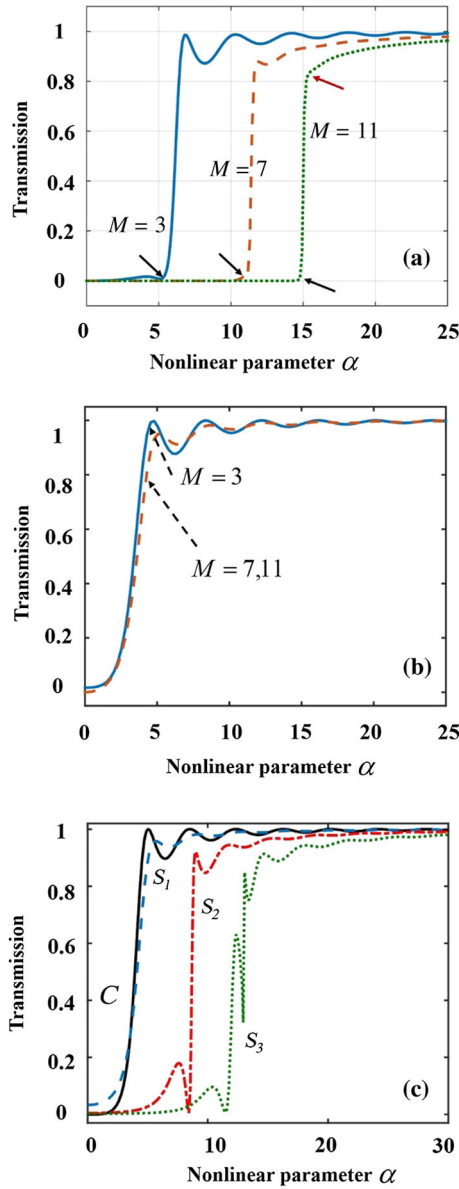
we also consider the case of edge coupling in a simple directional coupler case as well as the case of uniform arrays with three, seven, and eleven channels as depicted in Fig. 2(c). In the directional coupler case, we observe smooth but not very abrupt transition (the slope of the curve is ~16% of that of the case of the J_x array having eleven waveguide channels). For larger uniform arrays, we observe an interplay between sharp transitions and fast oscillations. Thus, based on the above simulations, we find that the nonlinear response of the J_x structures provides a superior performance in the sense that it is very abrupt and free of any oscillatory behavior. These results might find applications in several different photonic systems, as we will discuss later.

In order to illustrate the physics behind the observed abrupt transition between the off and on states [Fig. 2(a)], we investigate light-transport dynamics in a J_x photonic waveguide array made of seven guiding channels after a propagation distance $\xi = L \equiv \pi/2$ when light is launched in the leftmost channel. Under linear conditions $\alpha = 0$, we obtain coherent perfect transfer as expected [Fig. 3(a)]. As the nonlinear parameter increases, self-trapping effects take place and reduce the transmission to the rightmost port, as shown in Fig. 3(b) for $\alpha = 10$. However, in this regime, the nonlinear response is not strong enough to steer an appreciable optical energy to the leftmost channel from the adjacent waveguides. As the input light intensity is further increased, localization effects become stronger and just at $\alpha = 11.3$, transmission through the output port (leftmost
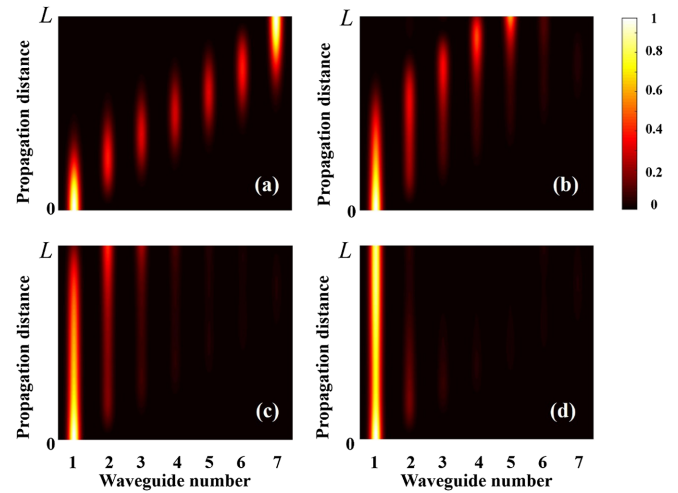

FIG. 3.   Light-transport dynamics in a nonlinear J_x array made of seven waveguides under different input light intensities as quantified by the value of the nonlinear parameter: (a) $\alpha = 0$, (b) $\alpha = 10$, (c) $\alpha = 11.3$, and (d) $\alpha = 12$. For a wide range of α, the self-trapping effects are not strong enough to prevent light diffraction and force the optical intensities to be confined in the same input channel. However, at a certain light-intensity threshold (defined in the text by α_{TH}), strong spatial soliton effects emerge, leading to a sudden and sharp increase in the transmission coefficient.

FIG. 2   (a) Transmission coefficient between the input and output ports as defined in Fig. 1 as a function of the nonlinear parameters (or input light intensity) for J_x arrays made of three, seven, and eleven waveguides, respectively. (b) A comparison with the performance of a uniform array as described in the text. Evidently, J_x arrays provide an abrupt transition between the off and on regimes—an effect that is not observed in uniform arrays. Note that the nonlinear response of the uniform array for $M = 7$ and 11 is almost identical. The black arrows in (a) indicate roughly the location of α_{TH} on each curve. The transition region is indicated on the $M = 11$ curve by the black and red arrows. (c) Nonlinear response under edge excitations in a simple directional coupler with coupling coefficient $\kappa_u = 1$ (curve C) and uniform arrays with seven waveguide channels when the coupling is $\kappa_u = 1$ (S_1), $\kappa_u = 2$ (S_2), and $\kappa_u = 3$ (S_3), respectively. In the directional coupler case, we observe smooth but not very abrupt (compared to the J_x array) transition. For larger uniform arrays, we observe a smooth transition for small coupling coefficients. As the coupling increases, the transition becomes sharper and is accompanied with fast oscillatory behavior.

channel) starts to rise as illustrated in Fig. 3(c). Finally, as shown in Fig. 3(d), at $\alpha = 12$ we observe strong spatial soliton effects where light remains mainly localized in the input waveguide and thus leads to a high-transmission coefficient. This same behavior is observed for arrays made of a different number of guiding elements with the difference that stronger nonlinearities (or higher light intensities) are needed to divert light from right to left when the number of the waveguides increases. This explains the behavior observed in Fig. 2(a), where the transmission curve shifts as a function of the number of the waveguides M. This last point is better illustrated in Fig. 4 where we quantify the dependence of α_{TH} and the sharpness of the transitions—defined by the slope of the transmission curve in the transition region (TR) and denoted by $(dT/d\alpha)_{TR}$ and computed by using a linear curve fitting at the central part of the transition region—as a function of the number of waveguides. Intuitively, one would expect that α_{TH} should scale with the coupling between the edge waveguide and the neighbor channel $g_{edge} = \sqrt{2N}$. Our numerical results confirm this prediction for large arrays. We also find that the slope $(dT/d\alpha)_{TR}$ follows a quadratic function with the array size to within 7%. These results hint at the possibility of semianalytical solutions for the nonlinear dynamics and surface soliton effects [42,43] that underline the nonlinear optical response of these structures, which we plan to investigate in detail elsewhere.

Intuitively, one would also expect other ports in the array (except the central one) to function as synthetic saturable absorbers. However, as shown in Fig. 5 for an array made of seven guiding channels, when light is launched and collected from port 2 or 3 (second leftmost waveguide or third leftmost one), interference effects become dominant in the transition region, giving rise to oscillatory
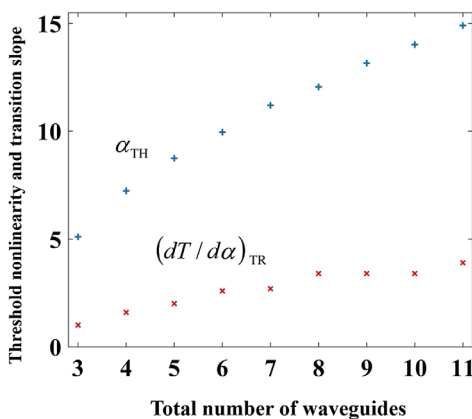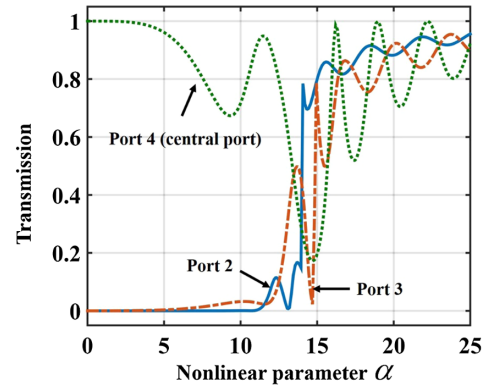

FIG. 5. Transmission dynamics in a J_x array made of seven waveguides as a function of the input light intensity when light is launched and collected from the same channel for waveguides number two, three, and four, respectively, after a normalized propagation distance of $\xi = L \equiv \pi/2$. Note that interference effects play an important role in these cases, leading to oscillatory behavior. When light is launched in the central channel, a low-transmission band (defined by intensity range rather than frequency range) exists between high-transmission bands—a feature that might find applications in laser systems.

transmission behavior before it eventually settles down. On the other hand, when light is launched in the central channel (waveguide number four in this example), the nonlinear response resembles that of a band-stop filter with a reduced
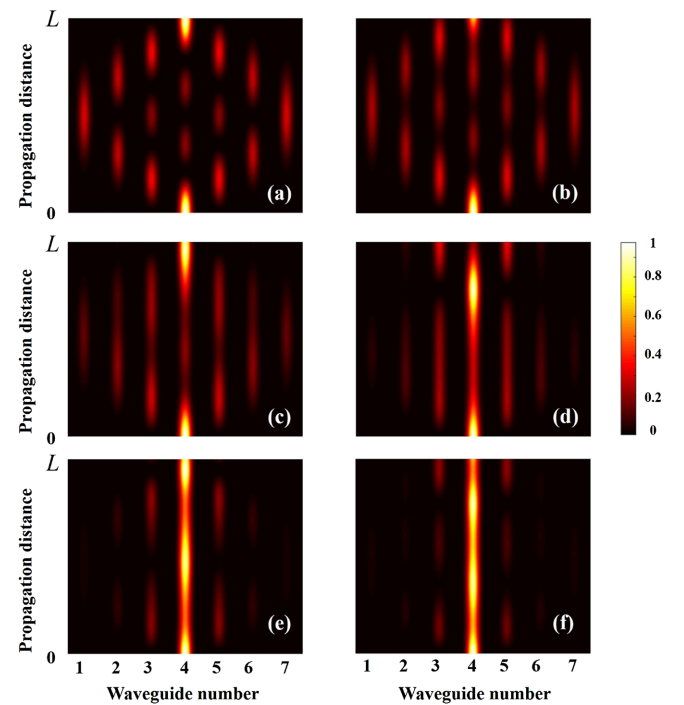

FIG. 4. The dependence of the threshold intensity characterized by α_{TH} and transition steepness defined by $(dT/d\alpha)_{\alpha_{TH}}$ on the array size. Our numerical results indicate that α_{TH} scales with the coupling between the edge waveguide and its neighbor channel $g_{edge} = \sqrt{2N}$. We also find that the slope $(dT/d\alpha)_{TR}$ follows a quadratic function with the array size to within 7%.

FIG. 6. Nonlinear wave propagation in the J_x array studied in Fig. 5 when light is excited at the central waveguide for $\alpha = 0, 9, 12, 14.5, 16.5,$ and 18, respectively are depicted in (a)–(f). From the plots, we can see that the interplay between nonlinear self-localization effects, reflection from the array edges, and interference lead to the oscillatory transmission behavior observed in Fig. 5.

transmission band between two high-transmission regions at very low and very high intensities—a feature that might find applications in controlling nonlinear laser dynamics. The nonlinear wave propagation dynamics that leads to the behavior observed in Fig. 5 are depicted in Fig. 6 for the case of central port excitation for different values of the nonlinear parameter α.

Now we briefly discuss several practical aspects of proposed synthetic saturable absorber structure. (1) *Experimental realization.*—We first note that linear J_x photonic arrays have been demonstrated in silica glass platforms [33]. Observing saturable absorption effects in these silica-based structures is possible at relatively higher optical intensities [41]. Another attractive alternative is to use (Al,Ga)As platforms which exhibit higher nonlinearities (almost 3 orders of magnitude higher than silica) [44] and are compatible with semiconductor laser technology—an advantage that might lead to integrating the laser device and the synthetic SA on the same chip to build microscale mode-locked lasers. (2) *Nonlinear response scaling.*—In addition to the predicted sharp "phase transition" between the low- and high-transmission modes (a feature that cannot be achieved by using uniform arrays) another advantage offered by our proposed structure is the ability to tailor the nonlinear response of the system by scaling the coupling constants between the waveguide elements without the need to employ a new material system. In addition, being a waveguide array-based device, the SA proposed in this work is expected to enjoy a relatively large bandwidth (a feature that we plan to investigate in future work by using full wave analysis). (3) *Ultrafast applications.*—Another interesting feature of the proposed device is that, similar to the work in Refs. [29–31], the absorption saturation effects rely on Kerr nonlinearity, which is an instantaneous effect that does not depend on any carrier relaxation mechanism and is thus suitable for ultrafast applications. We note that our analysis in this work is based on continuous-wave light-wave propagation. For ultrafast applications, one has to modify Eq. (1) to include temporal dispersion as well as additional nonlinear effects [41]. The details of these terms, however, are material and structure dependent and we will investigate them in detail in conjunction with specific material systems and particular photonic designs in future publications.

III. CONCLUSION

In conclusion, we explore a concept for building synthetic saturable absorbers based on photonic J_x arrays. We investigate the nonlinear response of these structures and we study their light-transport dynamics. Our simulations uncover an interesting behavior of sharp phase transition between two different transmission regimes: off and on states. This feature can be utilized to build on-chip mode-locked lasers as well as optical comparator devices that differentiate between zero and one states. Finally, test the robustness of the proposed device against possible fabrication errors by superimposing random perturbations over the values of the ideal coupling coefficients. The numerical results indicate that the nonlinear response function is very robust against 5% and even 10% disorder.

[1] R. El-Ganainy, K. G. Makris, D. N. Christodoulides, and Z. H. Musslimani, Theory of coupled optical $\mathcal{PT}$-symmetric structures, Opt. Lett. **32**, 2632 (2007).

[2] K. G. Makris, R. El-Ganainy, D. N. Christodoulides, and Z. H. Musslimani, Beam Dynamics in $\mathcal{PT}$ Symmetric Optical Lattices, Phys. Rev. Lett. **100**, 103904 (2008).

[3] Z. H. Musslimani, K. G. Makris, R. El-Ganainy, and D. N. Christodoulides, Optical Solitons in $\mathcal{PT}$ Periodic Potentials, Phys. Rev. Lett. **100**, 030402 (2008).

[4] A. Guo, G. J. Salamo, D. Duchesne, R. Morandotti, M. Volatier-Ravat, V. Aimez, G. A. Siviloglou, and D. N. Christodoulides, Observation of $\mathcal{PT}$-Symmetry Breaking in Complex Optical Potentials, Phys. Rev. Lett. **103**, 093902 (2009).

[5] C. E. Ruter, K. G. Makris, R. El-Ganainy, D. N. Christodoulides, M. Segev, and D. Kip, Observation of parity–time symmetry in optics, Nat. Phys. **6**, 192 (2010).

[6] H. Ramezani, T. Kottos, R. El-Ganainy, and D. N. Christodoulides, Unidirectional nonlinear $\mathcal{PT}$-symmetric optical structures, Phys. Rev. A **82**, 043803 (2010).

[7] B. Peng, S. K. Ozdemir, F. Lei, F. Monifi, M. Gianfreda, G. L. Long, S. Fan, F. Nori, C. M. Bender, and L. Yang, Parity–time-symmetric whispering-gallery microcavities, Nat. Phys. **10**, 394 (2014).

[8] H. Hodaei, M. A. Miri, M. Heinrich, D. N. Christodoulides, and M. Khajavikhan, Parity-time–symmetric microring lasers, Science **346**, 975 (2014).

[9] L. Feng, Z. J. Wong, R. M. Ma, Y. Wang, and X. Zhang, Single-mode laser by parity-time symmetry breaking, Science **346**, 972 (2014).

[10] L. Ge and R. El-Ganainy, Nonlinear modal interactions in parity-time ($\mathcal{PT}$) symmetric lasers, Sci. Rep. **6**, 24889 (2016).

[11] R. El-Ganainy, Li Ge, M. Khajavikhan, and D. N. Christodoulides, Supersymmetric laser arrays, Phys. Rev. A **92**, 033818 (2015).

[12] M. H. Teimourpour, L. Ge, D. N. Christodoulides, and R. El-Ganainy, Non-Hermitian engineering of single mode two dimensional laser arrays, Sci. Rep. **6**, 33253 (2016).

[13] J. Wiersig, Enhancing the Sensitivity of Frequency and Energy Splitting Detection by Using Exceptional Points: Application to Microcavity Sensors for Single-Particle Detection, Phys. Rev. Lett. **112**, 203901 (2014).

[14] R. El-Ganainy, J. I. Dadap, and R. M. Osgood, Optical parametric amplification via non-Hermitian phase matching, Opt. Lett. **40**, 5086 (2015).

[15] D. M. Finlayson and B. Sinclair, *Advances in Lasers and Applications* (CRC Press, London, 1999).

[16] R. Paschotta, *Field Guide to Laser Pulse Generation* (SPIE Press, Bellingham, WA, 2008).

[17] U. Keller, Recent developments in compact ultrafast lasers, Nature (London) **424**, 831 (2003).

[18] F. X. Kärtner and U. Keller, Stabilization of solitonlike pulses with a slow saturable absorber, Opt. Lett. **20**, 16 (1995).

[19] F. X. Kärtner and U. Keller, Stabilization of solitonlike pulses with a slow saturable absorber, Opt. Lett. **20**, 16 (1995).

[20] A. Isomaki, A.-M. Vainionpaa, J. Lyytikainen, and O. G. Okhotnikov, Semiconductor mirror for optical noise suppression and dynamic dispersion compensation, IEEE J. Quantum Electron. **39**, 1481 (2003).

[21] U. Keller, K. J. Weingarten, F. X. Kartner, D. Kopf, B. Braun, I. D. Jung, R. Fluck, C. Honninger, N. Matuschek, and J. Aus der Au, Semiconductor saturable absorber mirrors (SESAM's) for femtosecond to nanosecond pulse generation in solid-state lasers, IEEE J. Sel. Top. Quantum Electron. **2**, 435 (1996).

[22] E. U. Rafailov, M. A. Cataluna, and E. A. Avrutin, *Quantum Dot Saturable Absorbers, in Ultrafast Lasers Based on Quantum Dot Structures: Physics and Devices* (Wiley-VCH Verlag GmbH & Co. KGaA, Weinheim, Germany, 2011).

[23] S. V. Garnov, S. A. Solokhin, E. D. Obraztsova, A. S. Lobach, P. A. Obraztsov, A. I. Chernov, V. V. Bukin, A. A. Sirotkin, Y. D. Zagumennyi, Y. D. Zavartsev, S. A. Kutovoi, and I. A. Shcherbakov, Passive mode-locking with carbon nanotube saturable absorber in $Nd:GdVO_4$ and $Nd:Y_{0.9}Gd_{0.1}VO_4$ lasers operating at 1.34 μm, Laser Phys. Lett. **4**, 648 (2007).

[24] Q. Bao, H. Zhang, Y. Wang, Z. Ni, Y. Yan, Z. X. Shen, K. P. Loh, and D. Y. Tang, Atomic-layer graphene as a saturable absorber for ultrafast pulsed lasers, Adv. Funct. Mater. **19**, 3077 (2009).

[25] T. Brabec, Ch. Spielmann, P. F. Curley, and F. Krausz, Kerr lens mode locking, Opt. Lett. **17**, 1292 (1992).

[26] M. E. Fermann, F. Haberl, M. Hofer, and H. Hochreiter, Nonlinear amplifying loop mirror, Opt. Lett. **15**, 752 (1990).

[27] D. D. Hudson, K. Shish, T. R. Schibli, J. Nathan Kutz, D. N. Christodoulides, R. Morandotti, and S. T. Cundiff, Nonlinear femtosecond pulse reshaping in waveguide arrays, Opt. Lett. **33**, 1440 (2008).

[28] D. N. Christodoulides, F. Lederer, and Y. Silberberg, Discretizing light behaviour in linear and nonlinear waveguide lattices, Nature (London) **424**, 817 (2003).

[29] Joshua L. Proctor and J. Nathan Kutz, Passive mode-locking by use of waveguide arrays, Opt. Lett. **30**, 2013 (2005).

[30] J. Nathan Kutz and Björn Sandstede, Theory of passive harmonic mode-locking using waveguide arrays, Opt. Express **16**, 636 (2008).

[31] Q. Chao, D. D. Hudson, J. N. Kutz, and S. T. Cundiff, Waveguide array fiber laser, IEEE Photonics J. **4**, 1438 (2012).

[32] M. Christandl, N. Datta, T. C. Dorlas, A. Ekert, A. Kay, and A. J. Landahl, Perfect transfer of arbitrary states in quantum spin networks, Phys. Rev. A **71**, 032312 (2005).

[33] M. Bellec, G. M. Nikolopoulos, and S. Tzortzakis, Faithful communication Hamiltonian in photonic lattices, Opt. Lett. **37**, 4504 (2012).

[34] A. Perez-Leija, R. Keil, H. Moya-Cessa, A. Szameit, and D. N. Christodoulides, Perfect transfer of path-entangled photons in J_x photonic lattices, Phys. Rev. A **87**, 022303 (2013).

[35] S. Wiemann, A. Perez-Leija, M. Lebugle, R. Keil, M. Tichy, M. Grafe, R. Heimann, S. Noltel, H. Moya-Cessa, G. Wiehs, D. N. Christodoulides, and A. Szameit, Implementation of quantum and classical discrete fractional Fourier transforms, Nat. Commun. **7**, 11027 (2016).

[36] A. P. Perez-Leija, R. Keil, A. Kay, H. Moya-Cessa, S. Nolte, L.-C. Kwek, B. M. Rodríquez-Lara, A. Szameit, and D. N. Christodoulides, Coherent quantum transport in photonic lattices, Phys. Rev. A **87**, 012309 (2013).

[37] R. El-Ganainy, A. Eisfeld, M. Levy, and D. N. Christodoulides, On-chip non-reciprocal optical devices based on quantum inspired photonic lattices, Appl. Phys. Lett. **103**, 161105 (2013).

[38] R. El-Ganainy and M. Levy, On-chip multi 4-port optical circulators, IEEE Photonics J. **6**, 0600408 (2013).

[39] M. H. Teimourpour, D. N. Christodoulides, and R. El-Ganainy, Optical revivals in nonuniform supersymmetric photonic arrays, Opt. Lett. **41**, 372 (2016).

[40] M. H. Teimourpour, R. El-Ganainy, A. Eisfeld, A. Szameit, and D. N. Christodoulides, Light transport in $\mathcal{PT}$-invariant photonic structures with hidden symmetries, Phys. Rev. A **90**, 053817 (2014).

[41] G. Agrawal, *Nonlinear Fiber Optics* (Academic Press, London, 2012).

[42] K. G. Makris, S. Suntsov, D. N. Christodoulides, G. I. Stegeman, and A. Hache, Discrete surface solitons, Opt. Lett. **30**, 2466 (2005).

[43] S. Suntsov, K. G. Makris, D. N. Christodoulides, G. I. Stegeman, A. Haché, R. Morandotti, H. Yang, G. Salamo, and M. Sorel, Observation of Discrete Surface Solitons, Phys. Rev. Lett. **96**, 063901 (2006).

[44] R. El-Ganainy, S. Mokhov, K. G. Makris, D. N. Christodoulides, and R. Morandotti, Solitons in dispersion-inverted AlGaAs nanowires, Opt. Express **14**, 2277 (2006).